Supplementary Information

Unfunctionalized conjugated polymer microparticles for selective cancer cell imaging-guided photothermal therapy

Guangxue Feng,[ab] Jie Liu,[a] Junlong Geng,[a] and Bin Liu[ac]*

[a] Department of Chemical and Biomolecular Engineering, National University of Singapore, Singapore, 117585

[b] Environmental Research Institute, National University of Singapore, Singapore, 117411

[c] Institute of Materials Research and Engineering, 3 Research Link, Singapore, 117602

Correspondence and requests for materials should be addressed to B. Liu (email: cheliub@nus.edu.sg).

KEYWORDS: *Conjugated polymers, microparticles, fluorescence imaging, photothermal therapy, cancer cell detection*

Figure S1 shows the hydrodynamic diameter of PFBT NPs in aqueous. As shown, PFBT NPs exhibits a unimodal peak distribution with a narrow size variation ranges and a polydispersity of 0.151.

Figure S2 shows the entire absorption and emission spectra of PFBT NPs, PFTTQ NPs, and PFBT/PFTTQ co-loaded NPs and in aqueous solution. The first two peaks of the co-loaded NPs absorption spectrum originate from PFBT and PFTTQ, while the NIR peak is contributed by PFTTQ only. Based on the absorption intensity at 450 nm and 800 nm, it can be calculated that almost the same amounts of PFBT and PFTTQ were encapsulated by PLGA. As shown, co-loaded NPs showed similar fluorescence intensity as compared to that of PFBT NPs, indicating that the incorporation of PFTTQ in PFBT NPs will not affect the brightness of the particle.

Figure S3 shows the PFTTQ MPs morphology under confocal microscopy. It is noted that all the MPs are in the size of ~3 μm. However, it is difficult to distinguish PFTTQ from PLGA as both of them are non-fluorescence. Together with Figure 3, we confirmed the co-loading of PFBT and PFTTQ inside the same MPs through the fluorescent morphology changes.

Figure S4 shows the 3D confocal image of MCF-7 after treatment with PFBT MPs. The green fluorescence was observed from cell top to bottom inside the cytoplasm, indicating that PFBT MPs are internalized into cells, not attached to the cell surface.

Figure S5 shows the confocal images of U87MG and C6 cancer cells after treatment with PFBT MPs. Bright green fluorescence dots inside cell cytoplasm reveals that PFBT MPs possess the ability to internalize into other cancer cells.

Figure S6 represents the viabilities of MCF-7 cancer cells and NIH-3T3 cells after treatment with co-loaded CP MPs at different concentrations. The result shows over 80% viabilities for both cell lines, which indicates the excellent biocompatibility of our CP MPs to both cancer cells and normal cells.

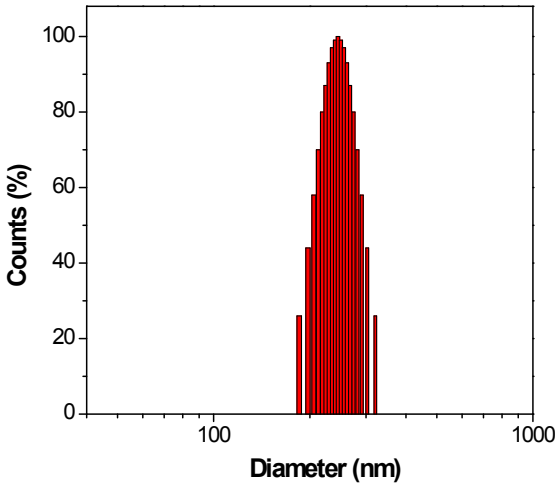

Figure S1. Size distribution of PFBT nanoparticles, measured by dynamic light scattering.

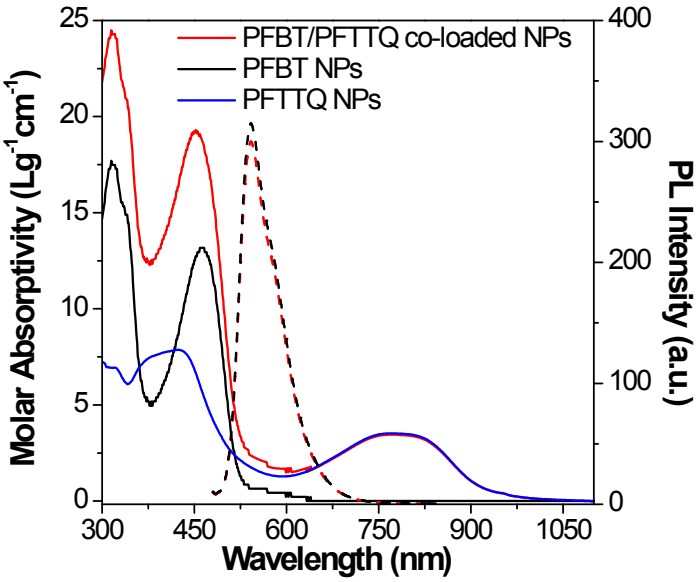

Figure S2. Absorption and fluorescence spectra of PFBT NPs, PFTTQ NPs, and PFBT and PFTTQ co-loaded NPs in aqueous solution. [CP NPs] = 0.01 mg/mL based on PFBT.

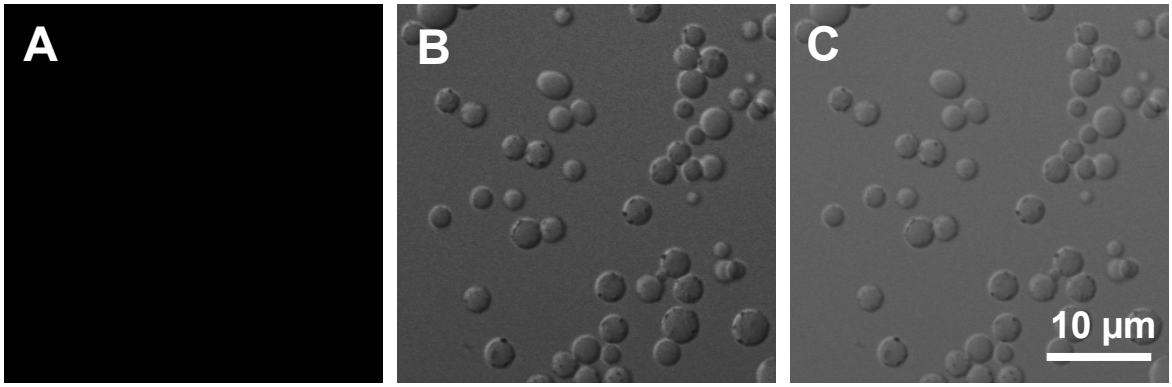

Figure S3. A) Fluorescence, B) white field, and C) fluorescence/white filed overlayed images of PFTTQ loaded CP MPs.

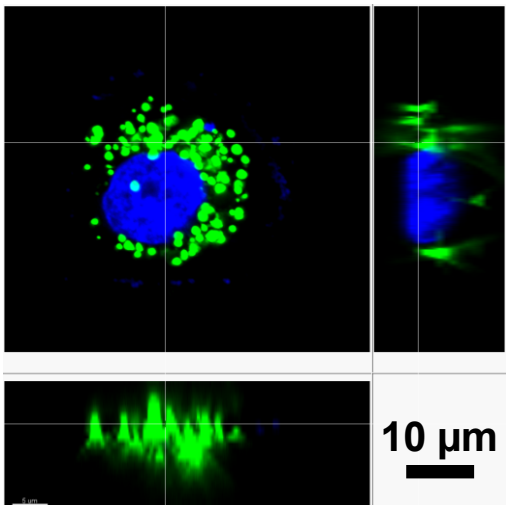

Figure S4. 3D CLSM image of PFBT MPs treated MCF-7 cells.

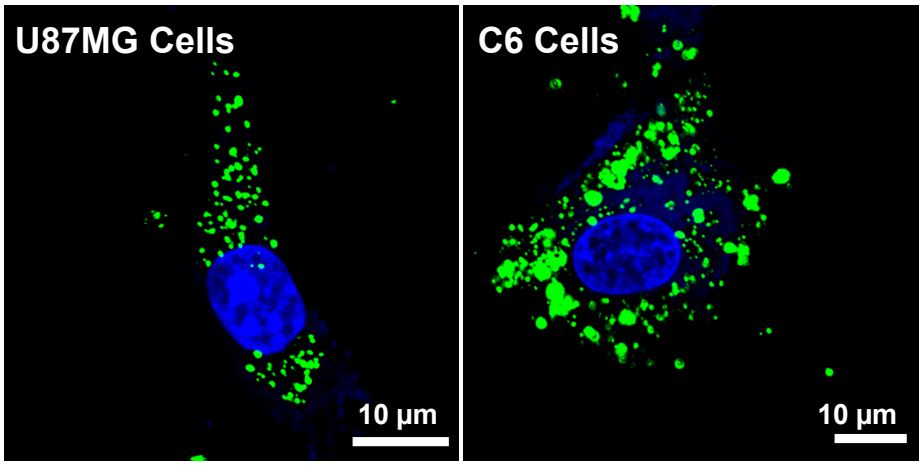

Figure S5. CLSM images of fluorescent CP MP treated U87MG and C6 cells.

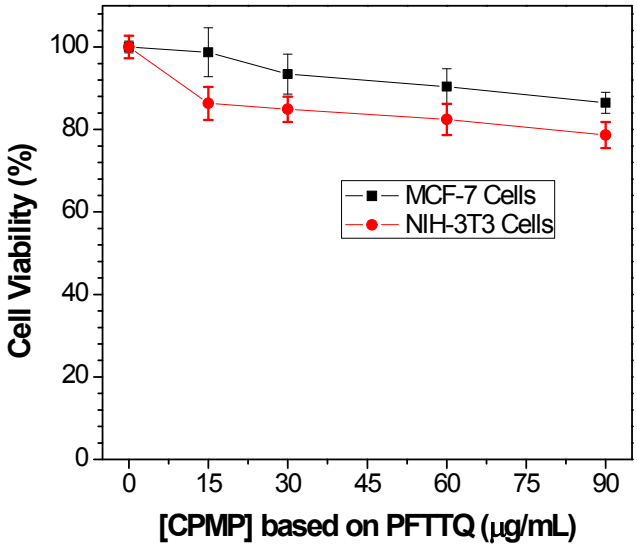

Figure S6. Cell viabilities of MCF-7 and NIH-3T3 cells after incubation with PFBT/PFTTQ co-loaded MPs at different concentrations, without NIR irradiation.